Spin Texture and Circular Dichroism in Photoelectron Spectroscopy from the Topological Insulator Bi_2Te_3: First-Principles Photoemission Calculations

H. Mirhosseini[1,*] and J. Henk[2,†]

[1]*Max Planck Institute of Microstructure Physics, Weinberg 2, D-06120 Halle (Saale), Germany*
[2]*Institute of Physics—Theoretical Physics, Martin Luther University Halle-Wittenberg, D-06099 Halle (Saale), Germany*
(Received 16 February 2012; published 20 July 2012)

By relativistic first-principles photoemission calculations for the topological insulator Bi_2Te_3, we study how the spin texture of the Dirac state manifests itself in circular dichroism. On one hand, there are significant modifications of the initial state's spin texture, which are explained by final-state effects and the symmetry of the photoemission setup. On the other hand, a highly symmetric setup allows us to draw conclusions about the detailed Dirac state's spin texture. Our study supports that circular dichroism in angular distribution successfully complements spin- and angle-resolved photoelectron spectroscopy from topological insulators.

Introduction.—Topological insulators are a new class of materials with promising properties for spintronic applications [1,2]. In particular, the three-dimensional topological insulators (TIs) of the binary-chalcogenide type Bi_2Se_3 and Bi_2Te_3 have gained a high level of interest [3]. Their Dirac surface state shows linear dispersion and exhibits a unique spin texture: The spin-orbit coupling leads to a chiral spin orientation in the constant energy contours (CECs) [4]. Further, warping in the CECs results in an out-of-plane tilting of the spin polarization [4–6]. This spin texture, derived by Fu from a model Hamiltonian [5], complies with most of the experimental data. However, first-principles calculations reveal a more complicated spin texture in Bi_2Te_3: a reversed spin orientation in the topmost Te layer and spin vortices at the cusps of heavily warped CECs. These features are attributed to hybridization with bulk states [7]. Furthermore, the degree of spin polarization in the Dirac state is significantly less than 100% [8]. Unconventional spin textures were also observed in photoelectron spectroscopy experiments [9,10].

Perhaps the most suitable way to determine the detailed spin texture in Bi_2Te_3 is spin-polarized and angle-resolved photoemission (SPARPES) [11] (see, for example, [12,13]). However, given the limited efficiency of today's spin detectors (e.g., [14]), one might instead use a spin-integrated technique, in particular circular dichroism in angular distribution (CDAD) (e.g., [15–17]), to gain the desired information [18]. Then, a question arises on how the spin texture manifests itself in the dichroic signal. Furthermore, the measured spin texture of the photoelectrons may deviate from that of the ground-state Dirac electron [19,20]. A reason is that the spin of the bound electron is altered by the spin of the incoming photon, as is expressed in the dipole-transition matrix elements. Also scattering effects in the final state may play a role. One might also ask whether the complicated layer-resolved spin texture, as is found in first-principles calculations [7], shows up in the photoemission spectra that comprise surface-sensitive but layer-integrated data. These

questions can be answered by state-of-the-art first-principles photoemission calculations in which all necessary ingredients (e.g., spin-orbit coupling, transition matrix elements, lifetimes, and multiple-scattering events) are fully taken into account. Such calculations provide a direct link between first-principles calculations for the initial state [21] and experiments.

In this Letter we report on such a theoretical investigation for Bi_2Te_3, focusing on the relation of spin texture and circular dichroism. On one hand, we find significant modifications of the initial state's spin texture, which are explained by final-state effects and the symmetry of the photoemission setup. On the other hand, we identify setups which allow us to draw conclusions about the detailed Dirac state's spin texture.

Computational aspects.—We only sketch our computational approach here; details are given in the online Supplemental Material [22]. Our density-functional-theory (DFT) calculations are performed within the relativistic layer–Korringa-Kohn-Rostoker method [23,24]. The exchange-correlation functional is taken from Perdew and Wang [25]. Detailed information on the atom- and spin-resolved electronic structure of semi-infinite Bi_2Te_3 is obtained from the Green function [26].

The self-consistent potentials from the DFT calculations serve as input for the computations of the spin- and angle-resolved photoemission intensities within the relativistic one-step model for semi-infinite systems [24,27]. This approach has proved successful in several studies of spin-orbit-interaction effects in SPARPES (e.g., [28]).

For our "computational experiments" we choose two setups. (1) The highly symmetric setup: For a photon energy of 21.22 eV, circularly polarized light [left-handed circularly polarized (LCP) and right-handed circularly polarized (RCP)] impinges in normal incidence; this is the standard CDAD setup with highest symmetry. (2) The experimental setup: For a photon energy of 8 eV, the light is incident oblique at a polar angle θ_{ph} of 40° and within the $\bar{K} - \bar{\Gamma} - \bar{K}$

azimuth (*xz* plane); this agrees with the setup of Jung *et al.* [6].

The Fermi levels in experiment and in theory often do not coincide due to doped samples. As a consequence, experiments can access initial states that are occupied in experiment but unoccupied in theory. Hence, we computed spectra for initial-state energies above E_F to come closer to experiments. As an alternative method to SPARPES, one might use inverse photoemission, which probes unoccupied states (e.g., [29,30]).

In the following we present photoemission intensities $I_\sigma(E, \mathbf{k}_\parallel)$ ($\sigma =$ LCP, RCP), their dichroism $\Delta I(E, \mathbf{k}_\parallel) \equiv I_{LCP}(E, \mathbf{k}_\parallel) - I_{RCP}(E, \mathbf{k}_\parallel)$, and spin differences $\mathbf{S}_\sigma(E, \mathbf{k}_\parallel) \equiv \mathbf{P}_\sigma(E, \mathbf{k}_\parallel) \cdot I_\sigma(E, \mathbf{k}_\parallel)$, where $\mathbf{P}$ is the photoelectrons spin polarization vector. Here k_x (k_y) is along the $\bar{K} - \bar{\Gamma} - \bar{K}$ ($\bar{M} - \bar{\Gamma} - \bar{M}$) line of the two-dimensional Brillouin zone. For the constant-initial-energy mode (CIS mode) we chose representative energies (here: E_F, $E_F + 100$ meV and $E_F + 250$ meV; E_F Fermi energy) to address the signatures of the spin texture in CECs with different warping [5]. We also calculated spectra in energy-distribution-curve (EDC) mode.

Highly symmetric setup.—In the CECs at E_F (Fig. 1, bottom row), bulk states appear at the six ray-like structures. The Dirac states manifests itself in the hexagonal shape, in which the CDAD is weak and shows threefold rotational symmetry. In the warped CECs at higher energies, however, the dichroism is increased (top rows): it is largest in the arcs and vanishes at the cusps. As we will see, this CDAD structure corresponds nicely to the texture of the spin polarization's *z* component S_z of the Dirac state. For the warped CECs we find an asymmetry within the arcs [marked by arrows in Figs. 1(a)–1(f)]; more specifically, the two arcs that cross the k_x axis show larger dichroism at $k_y > 0$ than for $k_y < 0$. This finding, which shows up in each of the six arcs, is attributed to the fcc(111)-type stacking sequence in each quintuple layer; the result is asymmetric scattering of the photoelectron. Recently, Scholz *et al.* [31] reported on CDAD results in which they have found an asymmetry pattern that is compatible with our findings.

"Optical orientation" is the alignment of the photoelectron spin along the helicity vector of the incident circular polarized light [32]. If the initial state is spin-polarized along the helicity vector—as is the Dirac state [5]—one observes dichroism (for magnetic systems, this effect is called magnetic circular dichroism [16,33]). Consequently, the texture of the dichroic signal reflects the spin texture of the spin-polarized initial state.

In a recent paper by Wang *et al.* [34], analytical expressions for the relation of spin texture and dichroic photoemission intensities are given. These show that the dichroism is sensitive to both the in-plane and perpendicular components of the initial state's spin, depending on the incidence direction of the circularly polarized light. Our quantitative findings are fully in line with these results.
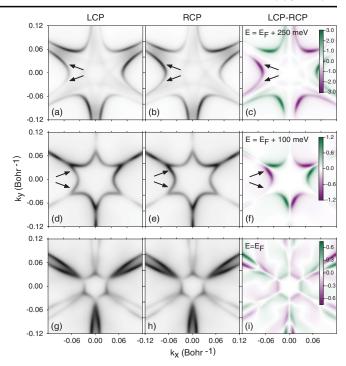

FIG. 1 (color).   Circular dichroism from Bi_2Te_3 in the high-symmetry setup for three selected energies, as indicated in each row (c), (f), (i). Left and center column: Intensities for LCP and RCP light, respectively, shown as gray scale. Right column: Intensity difference LCP-RCP, represented as color scale. Data for each energy share a common intensity scale. Arrows mark intensity asymmetries within selected arcs of the warped CECS (a)–(f) that are discussed in the text.

If photon spin and initial-state spin are parallel (antiparallel), the excitation probability is small (large), hence the dichroism upon reversal of the light helicity. This dichroism is accompanied by a small (large) *z* spin polarization of the photoelectron. This reasoning is nicely proven by the spin-resolved intensities for LCP and RCP light [Figs. 2(a) and 2(b)]. To be more precise, considering the LCP arcs that cross the k_x axis (marked by bold arrows) show small (large) intensity at $k_x < 0$ ($k_x > 0$); cf. Fig. 1(d). Consequently, the respective S_z's are small (almost white) or large (dark red); cf. Fig. 2(a). The opposite is true for RCP light [Figs. 1(e) and 2(b)].

While the CDAD is closely related to P_z, the in-plane components of the spin polarization are less affected by the light helicity (small arrows in Fig. 2). For both LCP and RCP light, the spin polarizations rotate clockwise along the CEC at E_F (bottom row), with a winding number of 1. At $E_F + 100$ meV (top row), the in-plane spin texture is more complicated because the surface parts of bulk states hybridize with the Dirac state at the cusps of the CEC, as was found in a recent calculation [7]. Since these electronic states are also affected by the spin-orbit interaction, they are spin-polarized but show a spin texture with a rotation direction opposite to that of the Dirac state. These lead to "spin vortices" at the cusps that also show up in the
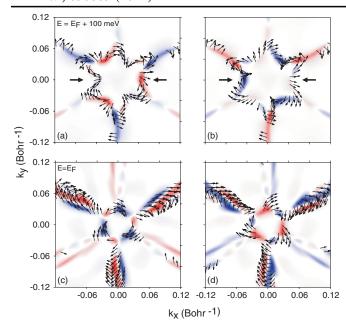
FIG. 2 (color). Spin textures in dichroic photoemission from Bi_2Te_3 in the high-symmetry setup for two selected initial energies, as indicated. Left (right) column: LCP (RCP) light. Top (bottom) row: E_F ($E_F + 100$ meV). The color scale represents the z component of the spin difference of the photoelectron, with (red, white, blue) = (negative, zero, positive) values. The in-plane xy components are visualized as small arrows. Bold arrows mark the arcs of the warped CECs (top row) that are discussed in the text.

FIG. 3 (color). Circular dichroism from Bi_2Te_3 in the experimental setup. Left (center): intensities for LCP (RCP) light, shown as gray scale (bright = weak intensity, dark = high intensity). Right: dichroic intensity, shown as color scale in arbitrary units. Arrows in the right panel indicate the sign change of the dichroism, found also in experiment [6]. The linear dispersion of the Dirac state is indicated by thin lines.

spin-resolved photoemission intensities; as a result, the winding number is 4.

Experimental setup.—The high-symmetry setup lends itself support to explain the major effects. However, it is seldom realized in real experiments. Therefore, we computed SPARPES intensities for a setup used in a recent experiment by Jung *et al.* [6]. The first striking result of Jung *et al.* was a reversal of the dichroic signal in one branch of the Dirac cone [at $k_x > 0$; cf. Fig. 1(d) in their publication]. Because the spin polarization of the initial state does not change sign with energy (as is given by Fu's model [5] and our first-principles calculation), this effect is explained as a final-state effect (including scattering of the outgoing photoelectron). Our calculations show the same change of sign in the branch at $k_x > 0$ but no change of sign in the branch at $k_x < 0$ (Fig. 3, marked by arrows). This agreement with the experiment implies that our calculations capture the essential details of the electronic structure. Further, a low-symmetry setup can result in asymmetric dichroic signals and spin textures, thus, making it difficult to conclude from the dichroic photoemission signal on the spin texture of the initial state.

As a consequence of the oblique light incidence, the intensity pattern—and likewise the CDAD—in the CECs becomes asymmetric (Fig. 4). The asymmetry shows up also in the spin texture. Nevertheless, it allows us to draw
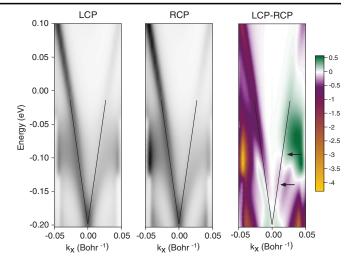
conclusions about the rotational direction which, strikingly, is reversed as compared to that in the high-symmetry setup. This finding is in particular astonishing because the rotation direction can be reversed by changing the azimuth of the light incidence [10]: We find a reversed direction for light impinging in the yz azimuth (not shown). The sign of the spin polarization's z component, however, is not affected.

A reversal of the spin texture may be brought about by the spin-orbit-influenced initial state. For the Rashba-split surface states of surface alloys (for example Bi/Ag(111) [35] or Bi/Cu(111) [36]), Park *et al.* showed theoretically [37] that the branch with $|j| = \frac{1}{2}$ (sp_z orbitals) exhibits a reversed spin texture as compared to that of the branch with $|j| = \frac{3}{2}$ (p_xp_y orbitals) that is due to the orbital angular momentum—a finding in contrast to the standard Rashba model. For Bi/Cu(111) we showed that hybridization among these $|j|$ branches can also result in a spin reversal [36]. The Dirac state in Bi_2Te_3 is a much more complicated mixture of p orbitals in the first quintuple layer as compared to the above nontopological surface states. Hence, it is obvious that the measured spin texture of the photoelectron depends—via transition matrix elements—on the very details of the setup.

While the asymmetry reversal in Bi_2Te_3 is reproduced by our theory, the CDAD signals at constant energies differ from their experimental counterparts (see Fig. 4 with Fig. 2 of Jung *et al.* [6]). With the data at hand, we can only speculate on the origin of these deviations. It appears that the theoretical intensity map is warped stronger in comparison to experiment; stronger warping is accompanied by a change in the spin texture [5] and therefore results in a different dichroic signal. Further, the n doping of the
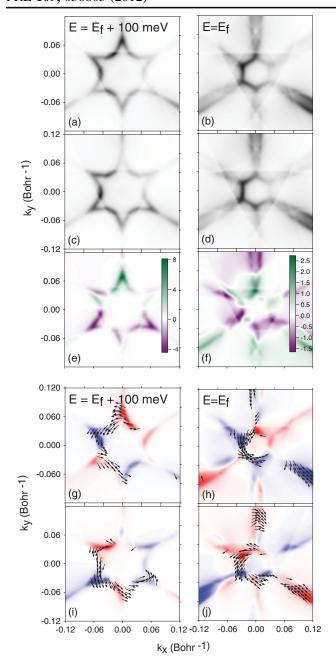
FIG. 4 (color). Circular dichroism and spin texture from Bi_2Te_3 in the experimental setup for two selected initial energies (left: $E_F + 100$ meV, right: E_F. The topmost columns show the CDAD as LCP and RCP intensities (grey scale) as well as the dichroic intensity (color scale). The two bottom columns depict the associated spin textures for LCP (g), (h) and RCP (i), (j) light, as in Fig. 2.

experimental samples could not only shift the Fermi level but also alter the spin texture with respect to undoped samples.

Conclusions.—Our investigations show that circular dichroism is a suitable method for analyzing the spin texture of the Dirac state in topological insulators, provided an appropriate setup is chosen. Since circular dichroism

mainly probes the out-of-plane component of the spin polarization, spin- and angle-resolved photoelectron spectroscopy is the method of choice for observing the in-plane components.

We are grateful to Changyoung Kim for fruitful discussions and for sending us data prior to publication.

*hossein@mpi-halle.mpg.de
†juergen.henk@physik.uni-halle.de

[1] H. Hasan and C. Kane, Rev. Mod. Phys. **82**, 3045 (2010).

[2] M. Z. Hasan and J. E. Moore, Annu. Rev. Condens. Matter Phys. **2**, 55 (2011).

[3] H. Zhang, C.-X. Liu, X.-L. Qi, Z. Fang, and S.-C. Zhang, Nature Phys. **5**, 438 (2009).

[4] S. Basak, H. Lin, L. A. Wray, S.-Y. Xu, L. Fu, M. Z. Hasan, and A. Bansil, Phys. Rev. B **84**, 121401 (2011).

[5] L. Fu, Phys. Rev. Lett. **103**, 266801 (2009).

[6] W. Jung, Y. Kim, B. Kim, Y. Koh, C. Kim, M. Matsunami, S.-i. Kimura, M. Arita, K. Shimada, J. H. Han, J. Kim, B. Cho, and C. Kim, Phys. Rev. B **84**, 245435 (2011).

[7] J. Henk, A. Ernst, S. V. Eremeev, E. C. Chulkov, I. V. Maznichenko, and I. Mertig, Phys. Rev. Lett. **108**, 206801 (2012).

[8] O. V. Yazyev, J. E. Moore, and S. G. Louie, Phys. Rev. Lett. **105**, 266806 (2010).

[9] D. Hsieh, Y. Xia, L. Wray, D. Quian, A. Pal, J. H. Dil, J. Osterwalder, F. Meier, G. Bihlmayer, C. L. Kane, Y. S. Hor, R. J. Cava, and M. Z. Hasan, Science **323**, 919 (2009).

[10] S.-Y. Xu, Y. Xia, L. A. Wary, S. Jia, F. Meier, J. H. Dil, J. Osterwalder, B. Slomski, A. Bansil, H. Lin, R. J. Cava, and M. Z. Hasan, Science **332**, 560 (2011).

[11] D. Hsieh, L. Wray, D. Qian, Y. Xia, J. H. Dil, F. Meier, L. Patthey, J. Osterwalder, G. Bihlmayer, Y. S. Hor, R. J. Cava, and M. Z. Hasan, New J. Phys. **12**, 125001 (2010).

[12] *Solid-State Photoemission and Related Methods. Theory and Experiment*, edited by W. Schattke and M. A. van Hove (Wiley-VCH, Weinheim, 2003).

[13] U. Heinzmann and J. H. Dil, J. Phys. Condens. Matter **24**, 173001 (2012).

[14] J. Kirschner, Appl. Phys. A **36**, 121 (1985).

[15] H. Ebert, J. Minár, and V. Popescu, in *Band-Ferromagnetism: Ground-State and Finite-Temperature Phenomena*, Lecture Notes in Physics Vol. 580, edited by K. Baberschke, W. Nolting, and M. Donath (Springer, Berlin, 2001) p. 371.

[16] *Spin-Orbit Influenced Spectroscopies of Magnetic Solids*, edited by H. Ebert and G. Schütz, Lecture Notes in Physics Vol. 466(Springer, Berlin, 1996).

[17] *Circular Dichroism. Principles and Applications*, edited by N. Berova, K. Nakanishi, and R. W. Woody (Wiley-VCH, New York, 2000), 2nd ed..

[18] S. R. Park, J. Han, C. Kim, Y. Y. Koh, C. Kim, H. Lee, H. J. Choi, J. H. Han, K. D. Lee, N. J. Hur, M. Arita, K. Shimada, H. Namatame, and M. Tamaguchi, Phys. Rev. Lett. **108**, 046805 (2012).

[19] C. Jozwiak, Y. L. Chen, A. V. Fedorov, J. G. Analytis, C. R. Rotundu, A. K. Schmid, J. D. Denlinger, Y.-D. Chuang,

D.-H. Lee, I. R. Fisher, R. J. Birgeneau, Z.-X. Shen, Z. Hussain, and A. Lanzara, Phys. Rev. B **84**, 165113 (2011).

[20] J. W. McIver, D. Hsieh, H. Steinberg, P. Jarillo-Herrero, and N. Gedik, Nature Nanotech. **7**, 96 (2012).

[21] W. Zhang, R. Yu, H.-J. Zhang, X. Dai, and Z. Fang, New J. Phys. **12**, 065013 (2010).

[22] See Supplemental Material at http://link.aps.org/supplemental/10.1103/PhysRevLett.109.036803 for details of the computations.

[23] *Electron Scattering in Solid Matter*, edited by J. Zabloudil, R. Hammerling, L. Szunyogh, and P. Weinberger (Springer, Berlin, 2005).

[24] J. Henk, in *Handbook of Thin Film Materials*, edited by H. S. Nalwa (Academic Press, San Diego, 2002), Vol. 2, Chap. 10, p. 479.

[25] J. P. Perdew and Y. Wang, Phys. Rev. B **45**, 13244 (1992).

[26] S. V. Eremeev, *et al.*, Nature Commun. **3**, 635 (2012).

[27] J. Braun, Rep. Prog. Phys. **59**, 1267 (1996).

[28] J. Henk, M. Hoesch, J. Osterwalder, A. Ernst, and P. Bruno, J. Phys. Condens. Matter **16**, 7581 (2004).

[29] P. D. Johnson and V. Dose, Rev. Sci. Instrum. **61**, 2277 (1990).

[30] M. Donath, Prog. Surf. Sci. **35**, 47 (1990).

[31] M. R. Scholz, D. Marchenko, A. Varykhalov, A. Volykhov, L. V. Yashina, and O. Rader, arXiv:1108.1053v1.

[32] J. Kessler, *Polarized Electrons*, Springer Series on Atoms and Plasmas (Springer, Berlin, 1985), Vol. 1, 2nd ed.

[33] W. Kuch, A. Dittschar, K. Meinel, M. Zharnikov, C. M. Schneider, J. Kirschner, J. Henk, and R. Feder, Phys. Rev. B **53**, 11621 (1996).

[34] Y. H. Wang, D. Hsieh, D. Pilon, L. Fu, D. R. Gardner, Y. S. Lee, and N. Gedik, Phys. Rev. Lett. **107**, 207602 (2011).

[35] C. R. Ast, J. Henk, A. Ernst, L. Moreschini, M. C. Falub, D. Pacilé, P. Bruno, K. Kern, and M. Grioni, Phys. Rev. Lett. **98**, 186807 (2007).

[36] H. Mirhosseini, J. Henk, A. Ernst, S. Ostanin, C.-T. Chiang, P. Yu, A. Winkelmann, and J. Kirschner, Phys. Rev. B **79**, 245428 (2009).

[37] S. R. Park, C. H. Kim, J. Yu, J. H. Han, and C. Kim, Phys. Rev. Lett. **107**, 156803 (2011).